Available online at www.sciencedirect.com
SCIENCE DIRECT®
Journal of Magnetic Resonance 177 (2005) 221–227
JMR Journal of Magnetic Resonance
www.elsevier.com/locate/jmr

# $R_{1\rho}$ relaxation for two-site chemical exchange: General approximations and some exact solutions

Vesselin Z. Miloushev, Arthur G. Palmer III *

*Department of Biochemistry and Molecular Biophysics, Columbia University, 630 West 168th Street, New York, NY 10032, USA*

Received 29 April 2005; revised 21 June 2005
Available online 6 September 2005

**Abstract**

Analytic expressions for the nuclear magnetic spin relaxation rate constant for magnetization spin-locked in the rotating reference frame under an applied radiofrequency field, $R_{1\rho}$, are obtained for two-site chemical exchange. The theoretical approach is motivated by Laguerre's method and obtains $R_{1\rho}$ as the root of a $(p_1, q_1)$ Padé approximant. The general formula for $R_{1\rho}$ obtained by this approach is substantially simpler than existing expressions and is equally or slightly more accurate, in most cases. In addition, particular solutions for the $R_{1\rho}$ rate constant are presented for two special cases: equal populations of the two exchanging sites, or placement of the radiofrequency carrier at the average resonance frequency of the two sites. The solutions are exact when the $R_1$ and $R_2$ relaxation rate constants are identical, and nearly exact under realistic experimental conditions.


*Keywords:* NMR spectroscopy; Rotating-frame relaxation; Chemical exchange; Laguerre's method; Pade approximation

## 1. Introduction

NMR spin relaxation in the rotating frame is a powerful method for characterizing dynamic processes in chemical and biological systems [1]. Recently, $R_{1\rho}$ relaxation dispersion experiments have been extended to describe systems using weak radiofrequency (rf) fields and slow chemical exchange kinetics [2–4]. As noted by Trott and Palmer [5], the $R_{1\rho}$ relaxation dispersion technique becomes more sensitive, compared to other techniques such as Carr–Purcell–Meiboom–Gill relaxation dispersion [6,7], to parameters characterizing chemical exchange processes at the extremes of slow exchange or weak rf fields. Characterizing such processes requires accurate analytical expressions for the $R_{1\rho}$ relaxation rate constant that are not limited to the fast-exchange regime and do not assume special experimental conditions, such as on-resonance irradiation [8,9].

Analytic expressions for the $R_{1\rho}$ relaxation rate constant for nuclear spins subject to $N$-site chemical exchange when the site populations are skewed, i.e., one site is much more highly populated than the others, have been obtained by analyzing the $3N \times 3N$ Bloch–McConnell equations [5,10]. For the simple case of two-site ($N = 2$) exchange, a series of increasingly accurate expressions for $R_{1\rho}$ have been obtained using the average magnetization approach, which treats the evolution of the average density operator in the stochastic Liouville equation (SLE); however, increased accuracy is been obtained at the cost of substantial algebraic complexity [1,11,12].

In this paper, we return to the description of $R_{1\rho}$ relaxation for chemical exchange of isolated nuclear spins between two sites with distinct magnetic environments, using the the Bloch–McConnell equations [10]. The $R_{1\rho}$ relaxation rate is the largest (least negative) real root of

* Corresponding author. Fax: +1 212 305 6949.
*E-mail address:* agp6@columbia.edu (A.G. Palmer).

1090-7807/$ - see front matter © 2005 Elsevier Inc. All rights reserved.
doi:10.1016/j.jmr.2005.07.023

the sixth-order characteristic polynomial derived from the $6 \times 6$ Bloch–McConnell evolution matrix. In general, the roots of a sixth-order polynomial cannot be expressed with a finite number of elementary arithmetic operations or root extractions [13]. However, this statement does not preclude solvable special cases, or approximate expressions of arbitrary accuracy. Motivated by Laguerre's method for polynomial root finding, we obtain a new analytical expression for the $R_{1\rho}$ relaxation rate constant. This general formula is substantially simpler and, in most cases, is equally or more accurate than expressions obtained using the average magnetization approach [1,11]. We also present a new expression for $R_{1\rho}$ that is valid for two special cases: equal site populations or placement of the rf carrier at the average resonance position. This expression is exact when the $R_1$ and $R_2$ relaxation rate constants are identical, and nearly exact under realistic experimental conditions, even if $R_1 \neq R_2$. The increased accuracy and algebraic simplicity of the new expressions for the $R_{1\rho}$ relaxation rate constant are important particularly for interpretation of experimental $R_{1\rho}$ relaxation dispersion data in chemical and biological systems, including proteins and other biomacromolecules.

## 2. Theory

### 2.1. Bloch–McConnell equations

For two-site exchange, under an applied rf field, the Bloch–McConnell equations describe evolution of the site magnetizations

$$\frac{\mathrm{d}}{\mathrm{d}t}\begin{bmatrix}\mathbf{M}_a(t)\\ \mathbf{M}_b(t)\end{bmatrix} = \left\{\begin{bmatrix}\mathbf{L}_a & 0\\ 0 & \mathbf{L}_b\end{bmatrix} + \mathbf{K}\otimes\mathbf{1}_s\right\}\begin{bmatrix}\mathbf{M}_a(t)\\ \mathbf{M}_b(t)\end{bmatrix}, \tag{1}$$

in which $\mathbf{M}_j(t) = [M_{xj}(t),\ M_{yj}(t), M_{zj}(t)]^{\mathrm{T}}$ is understood to represent the deviation of the magnetization associated with site $j = (a, b)$ away from the thermal equilibrium value,

$$\mathbf{L}_j = \begin{bmatrix}-R_{2j} & -\delta_j & 0\\ \delta_j & -R_{2j} & -\omega_1\\ 0 & \omega_1 & -R_{1j}\end{bmatrix}, \tag{2}$$

$$\mathbf{K} = \begin{bmatrix}-k_{ab} & k_{ba}\\ k_{ab} & -k_{ba}\end{bmatrix}, \tag{3}$$

and $\mathbf{1}_s$ is the $3 \times 3$ identity matrix. The resonance offset for site $j$, $\delta_j$, is defined as

$$\delta_j = \Omega_j - \omega_{\mathrm{rf}}, \tag{4}$$

in which $\Omega_j$ is the Larmor frequency of spins in site $j$, and $\omega_{\mathrm{rf}}$ is the frequency of the applied field; $R_{1j}$ and $R_{2j}$ are the site-specific spin–lattice and spin–spin relaxation rate constants, respectively, which arise from mechanisms other than chemical exchange, including dipole–dipole and chemical shift anisotropy mechanisms; $\omega_1$ is the amplitude of the applied rf field; The equilibrium site populations are $p_a = k_{ba}/(k_{ab} + k_{ba})$, $p_b = k_{ab}/(k_{ab} + k_{ba})$, where $k_{ij}$ is the microscopic reaction rate constant for exchange from site $i$ to site $j$, and $p_a \geqslant p_b$ is assumed. In the remainder of this paper, the expression in curly braces in Eq. (1) is called the Bloch–McConnell evolution matrix.

### 2.2. Previously derived expressions

An expression for the $R_{1\rho}$ relaxation rate constant applicable outside of the limit of fast exchange was initially derived by Trott and Palmer, by linearizing the characteristic polynomial of the Bloch–McConnell equations [10]. This expression is given by

$$R_{1\rho} = \bar{R}_1\cos^2\theta + \bar{R}_2\sin^2\theta + \frac{\sin^2\theta p_a p_b \delta^2 k}{\omega_a^2\omega_b^2/\omega_e^2 + k^2} \tag{5}$$

and is accurate when the populations of the two sites are highly skewed ($p_a \gg p_b$). In Eq. (5),

$$\begin{aligned}
&\delta = \delta_a - \delta_b, \\
&\bar{X} = p_a X_a + p_b X_b, \\
&\Delta\Omega = \bar{\Omega} - \omega_{\mathrm{rf}}, \\
&\omega_j^2 = \delta_j^2 + \omega_1^2, \\
&\omega_e^2 = \Delta\Omega^2 + \omega_1^2, \\
&\theta = \arctan(\omega_1/\Delta\Omega), \\
&k = k_{ab} + k_{ba}.
\end{aligned} \tag{6}$$

Expressions that are more accurate when the populations are less skewed were derived by Trott, Abergel, and Palmer by considering the long-time evolution of the average density operator in either the time or Laplace domains [1,11,12]. This approach reduces the $6 \times 6$ Bloch–McConnell matrix for the site magnetizations to a $3 \times 3$ evolution matrix for the average magnetization. The largest real eigenvalue of this matrix can be obtained exactly as the root of the cubic characteristic polynomial and is a highly accurate, but very complex, approximation to $R_{1\rho}$. More tractable approximate expressions are obtained by linearizing the characteristic polynomial, or by expansion of the average resolvent in the Laplace domain. The most accurate of these expressions is given by:

$$R_{1\rho} = \bar{R}_1\cos^2\theta + \bar{R}_2\sin^2\theta + \left(\frac{1}{\gamma}\right)\frac{\sin^2\hat{\theta} p_a p_b \delta^2 k}{\hat{\omega}_a^2\hat{\omega}_b^2/\hat{\omega}_e^2 + k^2 - 2\sin^2\hat{\theta} p_a p_b \delta^2 + (1-\gamma)\omega_1^2}, \tag{7}$$

in which

$$\begin{aligned}
&\gamma = 1 + p_a p_b \delta^2(\sigma^2 - k^2 + \omega_1^2)/(\sigma^2 + k^2 + \omega_1^2)^2, \\
&\sigma = p_b\delta_a + p_a\delta_b, \\
&\hat{\omega}_j^2 = \delta_j^2 + \gamma\omega_1^2, \\
&\hat{\omega}_e^2 = \Delta\Omega^2 + \gamma\omega_1^2, \\
&\hat{\theta} = \arctan(\sqrt{\gamma}\omega_1/\Delta\Omega).
\end{aligned} \tag{8}$$

### 2.3. Characteristic polynomial

As discussed by Trott and Palmer, the $R_{1\rho}$ relaxation rate constant is determined by the largest (least-negative) real eigenvalue of the Bloch–McConnell evolution matrix [10]. Equivalently, $R_{1\rho}$ is determined by the largest (least-negative) real root of the associated characteristic polynomial [10]. For algebraic simplicity in the following, and consistent with Eqs. (5) and (7), relaxation due to $R_1$ and $R_2$ processes is separated from the contribution due to chemical exchange broadening, $\Gamma_{\mathrm{ex}}$, by defining:

$$R_{1\rho} = \bar{R}_1 \cos^2\theta + \bar{R}_2 \sin^2\theta + \Gamma_{\mathrm{ex}}, \tag{9}$$

To obtain solutions for $\Gamma_{\mathrm{ex}}$, we consider the characteristic polynomial of the Bloch–McConnell evolution matrix in the absence of relaxation due to $R_1$ and $R_2$ processes:

$$P(x) = x^6 + a_5 x^5 + a_4 x^4 + a_3 x^3 + a_2 x^2 + a_1 x + a_0, \tag{10}$$

in which the coefficients of the polynomial are given by

$$\begin{aligned} a_5 &= 3k, \\ a_4 &= \omega_a^2 + \omega_b^2 + 3k^2, \\ a_3 &= k[k^2 + (2p_a + 1)\omega_a^2 + (2p_b + 1)\omega_b^2], \\ a_2 &= k^2(\omega_e^2 + 2p_a\omega_a^2 + 2p_b\omega_b^2) + \omega_a^2\omega_b^2, \\ a_1 &= k(k^2\omega_e^2 + \omega_a^2\omega_b^2), \\ a_0 &= \delta^2 k^2 p_a p_b \omega_1^2. \end{aligned} \tag{11}$$

Consequently, the exchange contribution to the $R_{1\rho}$ relaxation rate constant is obtained as:

$$\Gamma_{\mathrm{ex}} = -\mathbf{r}_s, \quad \text{where} \quad \mathbf{r}_s = \max\{x \in \mathbb{R} \| P(x) = 0\}. \tag{12}$$

As elaborated by Abergel and Palmer, such a separation of $R_1$ and $R_2$ processes from the effects of chemical exchange is valid under realistic experimental conditions for which the correlation time for overall rotational diffusion of the molecule, $\tau_c$, satisfies $\tau_c k \ll 1$, and the site-specific relaxation rate constants satisfy $|R_{1b} - R_{1a}| \ll k$, $|R_{2b} - R_{2a}| \ll k$, and $\bar{R}_2 - \bar{R}_1 \ll k$ [1,12]. This separation is exact, for any value of $k$, if $R_{1a} = R_{1b} = R_{2a} = R_{2b}$.

### 2.4. Laguerre approximation

To approximate $\mathbf{r}_s$, we apply Laguerre's method for polynomial root finding. We compute a single iteration of the Laguerre approximant [14], evaluated with an initial guess of zero,

$$\mathbf{r}_s = -\frac{M}{\max\{G_0 \pm \sqrt{(M-1)(MH_0 - G_0^2)}\}}, \tag{13}$$

in which $M = 6$ is the order of the polynomial, and

$$G_0 = \left.\frac{P(x)'}{P(x)}\right|_{x=0} = \frac{a_1}{a_0}, \tag{14}$$

$$H_0 = \left(\frac{P(x)'}{P(x)}\right)^2 - \left.\frac{P(x)''}{P(x)}\right|_{x=0} = \left(\frac{a_1}{a_0}\right)^2 - \frac{2a_2}{a_0}. \tag{15}$$

The choice of the positive sign maximizes the denominator, and leads to the following formula for $\mathbf{r}_s$,

$$\mathbf{r}_s = -\frac{6a_0}{a_1 + \sqrt{25a_1^2 - 60a_0a_2}}. \tag{16}$$

To simplify the Laguerre approximant, we linearize the radical in the denominator. The linearization yields an upper bound on the value of the radical in the denominator, and hence a lower bound to the Laguerre approximant. The linearized expression for $\mathbf{r}_s$ is,

$$\mathbf{r}_s = -\frac{a_0}{a_1 - a_2 a_0/a_1}. \tag{17}$$

As will be utilized below, the linearized expression for the real root near zero is independent of the order of the polynomial, $M$. Adding contributions from $R_1$ and $R_2$ processes, and making use of the identity,

$$p_a\omega_a^2 + p_b\omega_b^2 = \omega_e^2 + \delta^2 p_a p_b \tag{18}$$

leads to the final result:

$$R_{1\rho} = \bar{R}_1\cos^2\theta + \bar{R}_2\sin^2\theta + \frac{\sin^2\theta p_a p_b \delta^2 k}{\omega_a^2\omega_b^2/\omega_e^2 + k^2 - \sin^2\theta p_a p_b \delta^2 \left(1 + \frac{2k^2(p_a\omega_a^2 + p_b\omega_b^2)}{\omega_a^2\omega_b^2 + \omega_e^2 k^2}\right)}. \tag{19}$$

This expression approaches the expression for $R_{1\rho}$ given in Eq. (5), as the quantity $(a_2a_0/a_1^2) \to 0$, which occurs when $a_0/a_1 \ll k$.

The result given in Eq. (19) is one of the principal results of this paper. In most cases, this expression is equally or more accurate than previously derived expressions, including Eq. (7). The accuracy of Eq. (19) is illustrated in Figs. 1 and 2. Equally importantly, the expression for $R_{1\rho}$ in Eq. (19) is substantially simplier algebraically, because it lacks the numerous factors of $\gamma$ found in the average magnetization expression, Eq. (7).

The linearized Laguerre approximant to a root near zero, Eq. (17), can also be applied to the cubic polynomial obtained from the average magnetization approach. The resulting expression for $R_{1\rho}$ has improved accuracy, but is substantially more complicated, compared to Eqs. (7) and (19) (not shown), and thus does not have practical benefits.

The linearized expression, Eq. (17), also can be derived by considering the quadratic truncation of the sixth-order characteristic polynomial.

$$P(x) \approx a_2x^2 + a_1x + a_0. \tag{20}$$

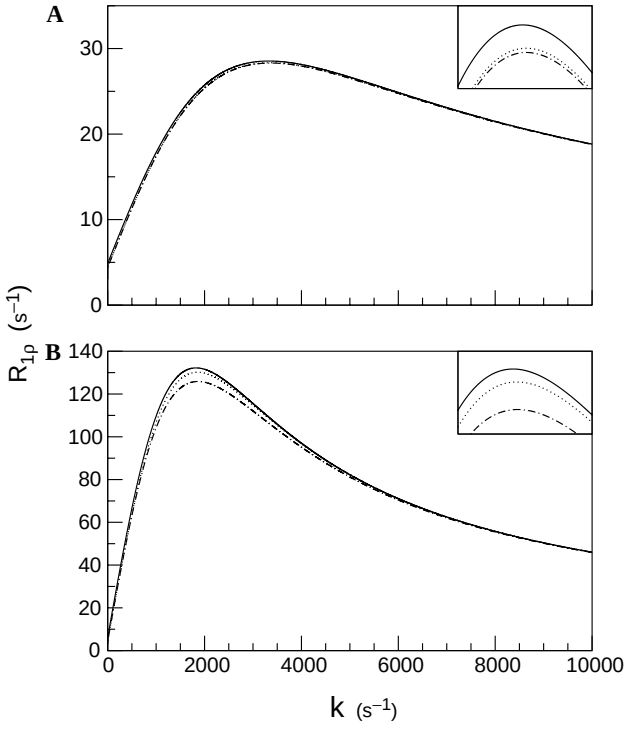


Fig. 1. Exchange rate dependence of the $R_{1\rho}$ relaxation rate constant. (—) Exact numerical largest real eigenvalue of the $6\times6$ Bloch–McConnell equations. (-·-) $R_{1\rho}$ as predicted by the average magnetization approximation, Eq. (7). (···) $R_{1\rho}$ as predicted by the linearized Laguerre approximant, Eq. (19). Parameters used in the calculations are: $\bar{R}_1 = 1.5\ s^{-1}$, $\bar{R}_2 = 11\ s^{-1}$, $\delta = 2400\ s^{-1}$, $\Delta\Omega = 1500\ s^{-1}$, and $\omega_1 = 1000\ s^{-1}$. (A) $p_a = 0.9$; inset shows the region of $k$ (2700, 4000), $R_{1\rho}$ (28, 28.7). (B) $p_a = 0.6$; inset shows the region of $k$ (1200, 2800), $R_{1\rho}$ (120, 135).

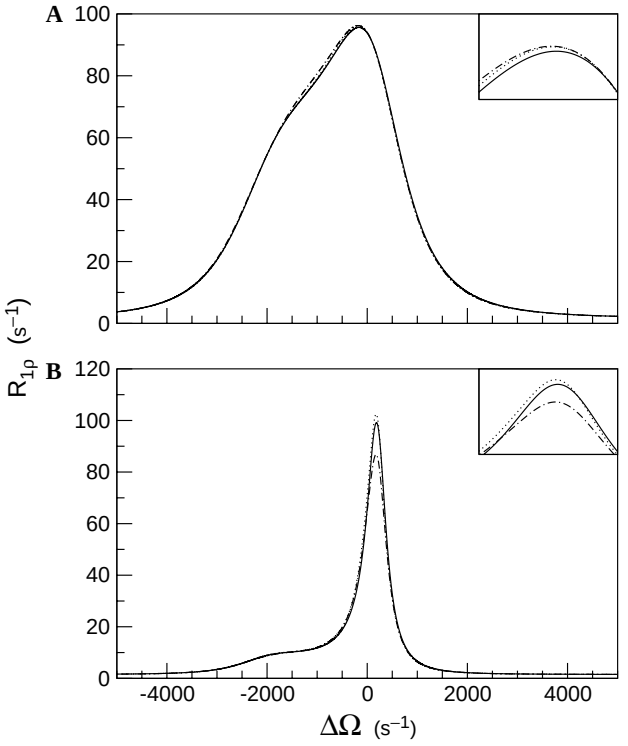


Fig. 2. Offset dependence of the $R_{1\rho}$ relaxation rate constant. (—) Exact numerical largest real eigenvalue of the $6\times6$ Bloch–McConnell equations. (-·-) $R_{1\rho}$ as predicted by the average magnetization approximation, Eq. (7). (···) $R_{1\rho}$ as predicted by the linearized Laguerre approximant, Eq. (19). Parameters used in the calculations are: $\bar{R}_1 = 1.5\ s^{-1}$, $\bar{R}_2 = 11\ s^{-1}$, $\delta = 2400\ s^{-1}$, $k = 1000\ s^{-1}$, and $p_a = 0.9$. (A) $\omega_1 = 1000\ s^{-1}$; inset shows the region of $\Delta\Omega$ (−500, 100), $R_{1\rho}$ (90, 100). (B) $\omega_1 = 250\ s^{-1}$; inset shows the region of $\Delta\Omega$ (−100, 400), $R_{1\rho}$ (50, 110).

Expressing the roots of the quadratic truncation using an alternate form of the quadratic equation [14], leads to,

$$\mathbf{r}_s = -\frac{2a_0}{a_1 \pm \sqrt{a_1^2 - 4a_0a_2}}. \tag{21}$$

This expression can be reduced to Eq. (17), by choosing the positive sign, and linearizing the radical in the denominator. We have opted, however, to derive the linearized formula using Laguerre approximation, because it is a more general method and also more accurate, as shown in Fig. 3.

### 2.5. Special case solutions

To simplify the characteristic polynomial in Eq. (10), we perform a linear Tschirnhausen transformation [13,15], by defining the new variable

$$x = y - \tfrac{1}{2}k \tag{22}$$

to eliminate the $a_5$ coefficient. Because the $a_5$ coefficient is the negative sum of the roots of the polynomial, such a transformation is equivalent to making the associated diagonal matrix of eigenvalues traceless. The resulting reduced polynomial is given by

$$P(y) = y^6 + b_4y^4 + b_3y^3 + b_2y^2 + b_1y + b_0, \tag{23}$$

in which

$$\begin{aligned}
b_4 &= \omega_a^2 + \omega_b^2 - \tfrac{3}{4}k^2, \\
b_3 &= k\Delta p(\omega_a^2 - \omega_b^2), \\
b_2 &= \tfrac{3}{16}k^4 + \tfrac{1}{4}k^2(\Delta p^2 - 1)(\omega_a^2 + \omega_b^2 - 2\omega_c^2) + \omega_a^2\omega_b^2, \\
b_1 &= -\tfrac{1}{4}k^3\Delta p(\omega_a^2 - \omega_b^2), \\
b_0 &= -\tfrac{1}{64}k^2[k^4 + 4k^2(\Delta p^2(\omega_a^2 + \omega_b^2 - 2\omega_c^2) + 2\omega_c^2) \\
&\quad + 16(\Delta p^2(\omega_a^2\omega_b^2 - \omega_c^4) + \omega_c^4)],
\end{aligned} \tag{24}$$

and the variables $\omega_c^2$ and $\Delta p$ have been introduced

$$\begin{aligned}
\omega_c^2 &= (\delta_a\delta_b + \omega_1^2), \\
\Delta p &= p_a - p_b.
\end{aligned} \tag{25}$$

The reduced polynomial can be solved as a cubic for $y^2$ provided that the coefficients $b_1$ and $b_3$ are zero. Excluding the trivial cases when $k = 0$, or $\Omega_a = \Omega_b$, this condition is satisfied when the populations of the two sites are equal, or when the carrier frequency, $\omega_{rf}$, is placed at the

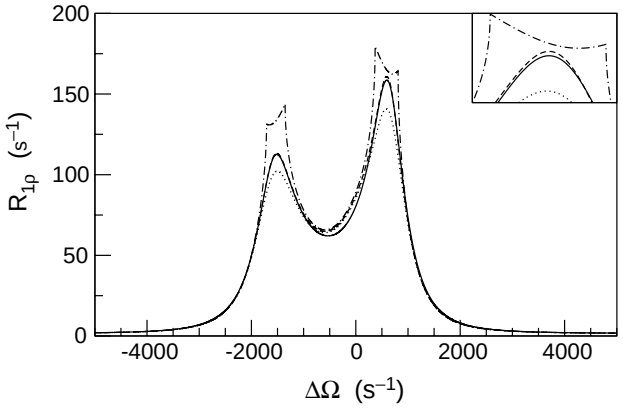


Fig. 3. Offset dependence of the $R_{1\rho}$ relaxation rate constant comparing the Laguerre approximant and the least-negative root of the truncated quadratic polynomial. (—) Exact numerical largest real eigenvalue of the $6\times6$ Bloch–McConnell equations. (···) $R_{1\rho}$ as predicted by the linearized Laguerre approximant, Eq. (19). (– – –) $R_{1\rho}$ with $\Gamma_{ex}$ as predicted by the Laguerre approximant, Eq. (16). (-·-) $R_{1\rho}$ with $\Gamma_{ex}$ as predicted by the least-negative root of the truncated quadratic polynomial, Eq. (21). The sharp transitions in the trace of Eq. (21) indicate a region where the approximation is no longer purely real. Parameters used in the calculations are: $\bar{R}_1 = 1.5\ s^{-1}$, $\bar{R}_2 = 11\ s^{-1}$, $\delta = 2400\ s^{-1}$, $k = 500\ s^{-1}$, $\omega_1 = 1000\ s^{-1}$, and $p_a = 0.7$; inset shows the region of $\Delta\Omega$ $(-300, 850)$, $R_{1\rho}$ $(135, 180)$.

numerical (not population-weighted) average resonance frequency of the two sites. We refer to these two cases as the *equal populations* or *average resonance frequency* conditions, respectively:

$$b_1 = b_3 = 0 \Leftarrow \begin{cases} \Delta p = 0 & : \quad p_a = p_b, \\ (\omega_a^2 - \omega_b^2) = 0 & : \quad \omega_{rf} = \frac{1}{2}(\Omega_a + \Omega_b). \end{cases} \tag{26}$$

To ensure that the desired real root is close to zero, we perform a second Tschirnhausen transformation by defining a new variable:

$$y^2 = z + \tfrac{1}{4}k^2. \tag{27}$$

Making this substitution and simplifying the coefficients leads to the cubic polynomial

$$P(z) = z^3 + c_2 z^2 + c_1 z + c_0, \tag{28}$$

in which

$$\begin{aligned} c_2 &= \omega_a^2 + \omega_b^2, \\ c_1 &= \omega_a^2\omega_b^2 + k^2\omega_e^2, \\ c_0 &= \delta^2 k^2 p_a p_b \omega_1^2. \end{aligned} \tag{29}$$

The three roots of this polynomial can be expressed with exact analytic formulas [14]. Using Eqs. (22) and (27), the six roots of Eq. (10) are given by

$$x = -k/2 \pm \sqrt{k^2/4 + z}, \quad \text{where} \quad P(z) = 0 \tag{30}$$

under the equal populations or average resonance frequency conditions. The resulting expression for $\Gamma_{ex}$ is given by

$$\begin{aligned} \Gamma_{ex} &= k/2 - \sqrt{k^2/4 + \mathbf{r}_c}, \quad \text{where} \\ \mathbf{r}_c &= \max\{z \in \mathbb{R} \| P(z) = 0\}. \end{aligned} \tag{31}$$

The exact expression for $\Gamma_{ex}$ is algebraically complex; to generate a more compact approximation, we consider the linearized Laguerre approximant at zero, as in Eq. (17), substituting the coefficients $c_k$ rather than $a_k$:

$$\Gamma_{ex} = k/2 - \sqrt{k^2/4 - \frac{c_0}{c_1 - c_2 c_0/c_1}}. \tag{32}$$

Adding the contribution from $R_1$ and $R_2$ processes and making explicit substitutions for the coefficients gives

$$R_{1\rho} = \bar{R}_1 \cos^2\theta + \bar{R}_2 \sin^2\theta + \frac{k}{2}\left(1 - \sqrt{1 - \frac{4\sin^2\theta p_a p_b \delta^2}{\omega_a^2\omega_b^2/\omega_e^2 + k^2 - \sin^2\theta p_a p_b \delta^2 \frac{k^2(\omega_a^2+\omega_b^2)}{\omega_a^2\omega_b^2+\omega_e^2 k^2}}}\right). \tag{33}$$

This expression is another principal result of this paper. It has improved performance compared to previous expressions, including the general approximation, Eq. (19), under the equal populations or average resonance frequency conditions. The accuracy of the expression in Eq. (33) is illustrated in Figs. 4 and 5.

## 3. Methods

Symbolic calculation of the characteristic polynomial for the Bloch–McConnell equations, Eqs. (1) and (10), and the simplification of coefficients in Eq. (24), were performed with Mathematica (Wolfram Research). Numerical simulations were performed with Scilab (Scilab Consortium, INRIA, ENPC). Figures were prepared with Scilab and Grace (http://plasma-gate.weizmann.ac.il/Grace/).

## 4. Discussion and conclusion

Motivated by Laguerre's method, we have derived new expressions for the $R_{1\rho}$ relaxation rate constant for nuclear spin magnetization locked by an rf field along the direction of the effective magnetic field in the rotating reference frame. Laguerre's method is a powerful root finding algorithm, which is guaranteed to iteratively converge to a complex root [14]. Indeed, single iterations of Laguerre's method can be used to obtain approximations to $R_{1\rho}$ or even $R_{2\rho}$, provided initial guesses are taken respectively at zero, or $\pm i\omega_a$. The resulting expression for $R_{2\rho}$, however, is complicated and accurate only for skewed populations, relatively higher field strengths, and higher exchange rates (not shown).

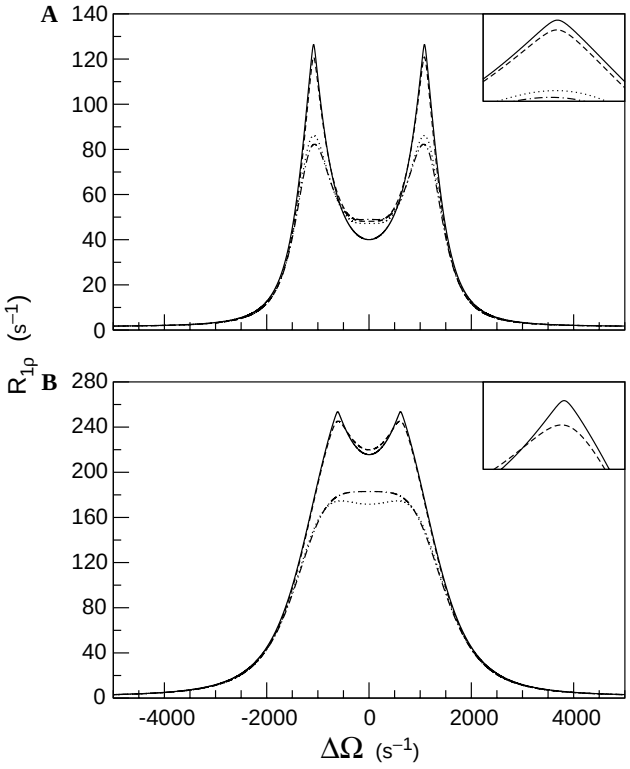


Fig. 4. Offset dependence of the $R_{1\rho}$ relaxation rate constant for equal site populations, $p_a = p_b$. (—) Exact numerical largest real eigenvalue of the $6 \times 6$ Bloch–McConnell equations. (-·-) $R_{1\rho}$ as predicted by the average magnetization approximation, Eq. (7). (···) $R_{1\rho}$ as predicted by the linearized Laguerre approximant, Eq. (19). (–––) $R_{1\rho}$ as predicted by Eq. (33). Parameters used in the calculations are: $\bar{R}_1 = 1.5\ s^{-1}$, $\bar{R}_2 = 11\ s^{-1}$, and $\delta = 2400\ s^{-1}$. (A) $k = 500\ s^{-1}$, $\omega_1 = 1000\ s^{-1}$; inset shows the region of $\Delta\Omega$ (300,850), $R_{1\rho}$ (230,260). (B) $k = 250\ s^{-1}$, $\omega_1 = 500\ s^{-1}$; inset shows the region of $\Delta\Omega$ (900,1250), $R_{1\rho}$ (80,130).

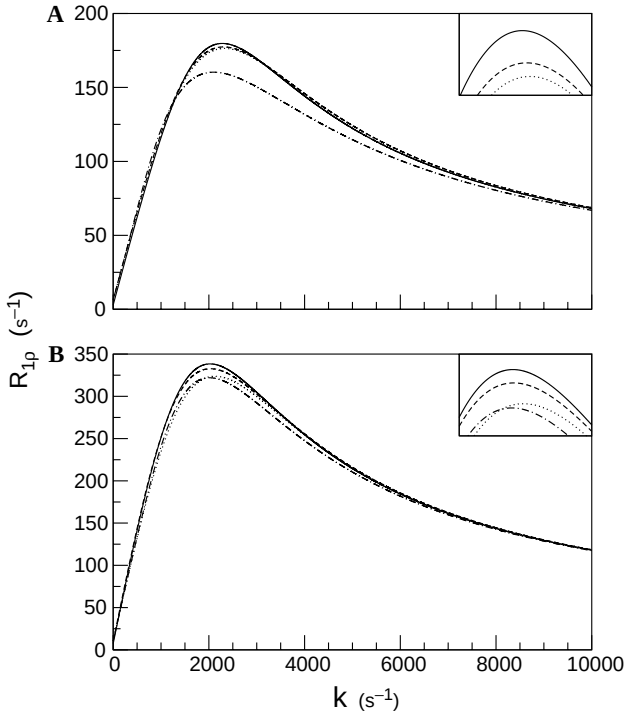


Fig. 5. Exchange rate dependence of the $R_{1\rho}$ relaxation rate constant for $\omega_{rf}$ set to the average resonance frequency. (—) Exact numerical largest real eigenvalue of the $6 \times 6$ Bloch–McConnell equations. (-·-) $R_{1\rho}$ as predicted by the average magnetization approximation, Eq. (7). (···) $R_{1\rho}$ as predicted by the linearized Laguerre approximant, Eq. (19). (–––) $R_{1\rho}$ as predicted by Eq. (33). Parameters used in the calculations are: $\bar{R}_1 = 1.5\ s^{-1}$, $\bar{R}_2 = 11\ s^{-1}$, $\delta = 2400\ s^{-1}$, and $p_a = 0.7$. (A) $\omega_1 = 500\ s^{-1}$; inset shows the region of $k$ (1900,2700), $R_{1\rho}$ (175,181). (B) $\omega_1 = 1500\ s^{-1}$; inset shows the region of $k$ (1500,2800), $R_{1\rho}$ (310,345).

In the present application, $R_{1\rho}$ was obtained by first computing the Laguerre approximant to the chemical exchange broadening contribution, $\Gamma_{ex}$, at zero, Eq. (16). The expression is simplified by linearizing the radical in the Laguerre approximant, Eq. (17). The linearized expression also can be obtained by considering the quadratic truncation of the characteristic polynomial. Adding contributions from $R_1$ and $R_2$ processes leads to the new expression for $R_{1\rho}$, Eq. (19). This expression has lower relative algebraic complexity compared to the average magnetization approximation, Eq. (7), while being equally or slightly more accurate in most cases.

The accuracy of the Laguerre approximant, Eq. (16), and linearized expression, Eq. (17), depends in a complicated manner on the resonance offsets, site populations, exchange rate constant, and applied field strength. Numerical simulations indicate that both expressions are accurate under most combinations of parameters if $p_a \geqslant 0.7$; for $p_a < 0.7$, the accuracy is reduced for slow exchange and/or weak rf fields. In addition, the Laguerre approximant performs better when $\omega_1 \geqslant k$; however, the linearized expression is more accurate for $\omega_1 < k$. In the latter circumstance, the Laguerre approximant tends to overestimate the $R_{1\rho}$ relaxation rate constant, or fails to converge to a real root.

The linearized expression, Eq. (17), is the root of a $(p_1, q_1)$ Padé approximant to the characteristic polynomial [16,17]. Specifically, the linearized expression is the root of the ratio of monomials, $p_1$ and $q_1$, that approximates the characteristic polynomial at zero. In a sense, the $(p_1, q_1)$ Padé approximant provides improved modeling of the characteristic polynomial at zero, extending the initial results of Trott and Palmer [10]. Higher order $(p_1, q_m)$ Padé approximants give improved results under some circumstances, at the cost of increased complexity.

Finally, an expression for $\Gamma_{ex}$, the chemical exchange broadening contribution to the $R_{1\rho}$ relaxation rate constant, Eq. (31), has been obtained for two special cases: equal site populations or placement of the rf carrier frequency at the average resonance position. The resulting expression for $R_{1\rho}$ is exact when the $R_1$ and $R_2$ relaxation rate constants are identical, and nearly exact when $\bar{R}_2 - \bar{R}_1 \ll k$. We also have applied the linearized expression, Eq. (17), to Eq. (31), finding a simple expression

with high accuracy, for these special cases, Eq. (33). The special case of equal site populations arises for systems exhibiting symmetric exchange, such as 180° rotations of aromatic rings in proteins [18–20]. Furthermore, for symmetric exchange, the average resonance frequency can be identified by direct inspection of the NMR spectrum.

The number of applications of $R_{1\rho}$ relaxation dispersion experiments for characterizing slow timescale dynamics in proteins and other biomacromolecules has increased dramatically over the past few years [2–4]. The highly accurate, algebraically simple, expressions presented in this paper will facilitate data analysis of $R_{1\rho}$ relaxation dispersion experiments, for systems in slow-to-intermediate exchange, at lower applied rf field strengths, and with site populations that are not highly skewed.

## Acknowledgments

Support from National Institutes of Health Grants MSTP 5T32 GM07367 (V.Z.M.) and GM59273 (A.G.P) are gratefully acknowledged. We thank Mark Rance (Univ. Cincinnati) for helpful discussions.

## References

[1] A.G. Palmer, NMR characterization of the dynamics of biomacromolecules, Chem. Rev. 104 (2004) 3623–3640.
[2] F. Massi, E. Johnson, C. Wang, M. Rance, A.G. Palmer, NMR $R_{1\rho}$ rotating-frame relaxation with weak radio frequency fields, J. Am. Chem. Soc. 126 (2004) 2247–2256.
[3] D.M. Korzhnev, V.Y. Orekhov, F.W. Dahlquist, L.E. Kay, Off resonance $R_{1\rho}$ relaxation outside of the fast exchange limit: an experimental study of a cavity mutant of T4 lysozyme, J. Biomol. NMR 26 (2003) 39–48.
[4] D.M. Korzhnev, V.Y. Orekhov, L.E. Kay, Off-resonance $R_{1\rho}$ NMR studies of exchange dynamics in proteins with low spin-lock fields: an application to a Fyn SH3 domain, J. Am. Chem. Soc. 127 (2005) 713–721.
[5] O. Trott, A.G. Palmer, Theoretical study of $R_{1\rho}$ rotating-frame and $R_2$ free-precession relaxation in the presence of $n$-site chemical exchange, J. Magn. Reson. 170 (2004) 104–112.
[6] H.Y. Carr, E.M. Purcell, Effects of diffusion on free precession in nuclear magnetic resonance experiments, Phys. Rev. 94 (1954) 630–638.
[7] S. Meiboom, D. Gill, Modified spin-echo method for measuring nuclear relaxation times, Rev. Sci. Instrum. 29 (1958) 688–691.
[8] D.G. Davis, M.E. Perlman, R.E. London, Direct measurements of the dissociation-rate constant for inhibitor–enzyme complexes via $T_{1\rho}$ and $T_2$ (CPMG) methods, J. Magn. Reson. Ser. B 104 (1994) 266–275.
[9] S. Meiboom, Nuclear magnetic resonance study of the proton transfer in water, J. Chem. Phys. 34 (1961) 375–388.
[10] O. Trott, A.G. Palmer, $R_{1\rho}$ relaxation outside the fast-exchange limit, J. Magn. Reson. 154 (2002) 157–160.
[11] O. Trott, D. Abergel, A.G. Palmer, An average-magnetization analysis of $R_{1\rho}$ relaxation outside of the fast exchange limit, Mol. Phys. 101 (2003) 753–763.
[12] D. Abergel, A.G. Palmer, On the use of the stochastic Liouville equation in NMR: application to $R_{1\rho}$ relaxation in the presence of exchange, Concept Magn. Reson. A 19 (2003) 134–148.
[13] R. King, Beyond the Quartic Equation, Birkhauser, Basel, 1996.
[14] W.H. Press, S.A. Teukolsky, W.T. Vetterling, B.P. Flannery, Numerical Recipes in FORTRAN, second ed., Cambridge University Press, Cambridge, 1992.
[15] V.S. Adamchik, D.J. Jeffrey, Polynomial transformations of Tschirnhaus, Bring and Jerrard, ACM SIGSAM Bull. 37 (2003) 90–93.
[16] A. Nourein, Root determination by use of Padé approximants, BIT 16 (1976) 291–297.
[17] T. Sakurai, T. Torii, H. Suguira, An iterative method for algebraic equation by Padé-approximation, Computing 46 (1991) 131–141.
[18] K. Wüthrich, G. Wagner, NMR investigations of the dynamics of the aromatic amino acid residues in the basic pancreatic trypsin inhibitor, FEBS Lett. 50 (1975) 265–268.
[19] G. Wagner, D. Brühwiler, K. Wüthrich, Reinvestigation of the aromatic side-chains in the basic pancreatic trypsin inhibitor by heteronuclear two-dimensional nuclear magnetic resonance, J. Mol. Biol. 196 (1987) 227–231.
[20] J.J. Skalicky, J.L. Mills, S. Sharma, T. Szyperski, Aromatic ring-flipping in supercooled water: implications for NMR based structural biology of proteins, J. Am. Chem. Soc. 123 (2001) 388–397.